

Influence of Fibroin Membrane Composition and Curing Parameters on the Performance of a Biodegradable Enzymatic Biosensor Manufactured from Silicon-Free Carbon

Kevin A. Janus, Stefan Achtsnicht, Laura Tempel, Aleksander Drinic, Alexander Kopp, Michael Keusgen, and Michael J. Schöning*

Herein, fibroin, polylactide (PLA), and carbon are investigated for their suitability as biocompatible and biodegradable materials for amperometric biosensors. For this purpose, screen-printed carbon electrodes on the biodegradable substrates fibroin and PLA are modified with a glucose oxidase membrane and then encapsulated with the biocompatible material Ecoflex. The influence of different curing parameters of the carbon electrodes on the resulting biosensor characteristics is studied. The morphology of the electrodes is investigated by scanning electron microscopy, and the biosensor performance is examined by amperometric measurements of glucose (0.5–10 mM) in phosphate buffer solution, pH 7.4, at an applied potential of 1.2 V versus a Ag/AgCl reference electrode. Instead of Ecoflex, fibroin, PLA, and wound adhesive are tested as alternative encapsulation compounds: a series of swelling tests with different fibroin compositions, PLA, and Ecoflex has been performed before characterizing the most promising candidates by chronoamperometry. Therefore, the carbon electrodes are completely covered with the particular encapsulation material. Chronoamperometric measurements with H₂O₂ concentrations between 0.5 and 10 mM enable studying the leakage current behavior.


products, like glucose, urea, and dopamine.^[4–8] When applying such sensors on human skin, the usage of skin-friendly, noninflammatory materials is mandatory.^[9,10] This led to a series of studies on biocompatible synthetic materials such as polylactide (PLA), polycaprolactone (PCL), polyethylene glycol (PEG), poly(vinyl alcohol) (PVA), and poly(3,4-ethylenedioxythiophene)-polystyrene sulfonate (PEDOT:PSS) for their application in biosensors.^[11–17] The inherent biocompatibility of natural materials (e.g., chitosan, collagen, hyaluronic acid, alginates, and gelatin) makes them promising candidates, too.^[18–21] Although, both natural and synthetic materials have been used in medical applications for many years, foreign body reactions (inflammation), fibrous encapsulation, or biofouling might occur, which will negatively influence the overall sensor performance.^[22,23]

In this context, scientists have rediscovered silk as a material for constructing “green” and harmless electronics.^[24] Silk, derived from the silkworm *Bombyx mori*, combines advantageous biocompatibility and time-adjustable biodegradability under physiological conditions with superior mechanical properties such as flexibility, high tensile strength, and high elongation at break.^[25] Fibroin is obtained from

1. Introduction

Interest in biocompatible and biodegradable electronic devices for medical applications has increased in recent years.^[1–3] Sensoric applications include, for example, the determination of ions such as sodium and potassium, pH, or metabolic

K. A. Janus, S. Achtsnicht, L. Tempel, M. J. Schöning
Institute of Nano- and Biotechnologies (INB)
FH Aachen
Campus Jülich, 52428 Jülich, Germany
E-mail: schoening@fh-aachen.de

 The ORCID identification number(s) for the author(s) of this article can be found under <https://doi.org/10.1002/pssa.202300081>.

© 2023 The Authors. physica status solidi (a) applications and materials science published by Wiley-VCH GmbH. This is an open access article under the terms of the Creative Commons Attribution-NonCommercial License, which permits use, distribution and reproduction in any medium, provided the original work is properly cited and is not used for commercial purposes.

DOI: 10.1002/pssa.202300081

K. A. Janus, M. Keusgen
Institute for Pharmaceutical Chemistry
Philipps University of Marburg
35032 Marburg, Germany

A. Drinic, A. Kopp
Fibrothelium GmbH
52068 Aachen, Germany

M. J. Schöning
Institute of Biological Information Processing (IBI-3)
Forschungszentrum Jülich GmbH
52425 Jülich, Germany

degummed silk and can be modified to create different morphologies, like sponges, gels, powders, scaffolds, membranes, or fibers.^[26] It is often discussed as a base material for the development of biocompatible devices, for example, as a substrate for flexible pressure, temperature, and humidity sensors, electrical gas sensors, thin-film graphene field-effect transistors, transient memristors, or thermally triggered drug delivery devices.^[27–31] Fibroin has been also suggested as a biocompatible interface to immobilize enzymes on a glassy carbon electrode to detect ascorbic acid or organophosphates and carbamates.^[32,33] Biocompatible electronics have been transferred to various surfaces such as teeth, eggs, or feline brain due to the adjustable water solubility of the fibroin membrane.^[34–36]

Our group recently introduced fibroin as a biocompatible and biodegradable substrate for an amperometric glucose biosensor.^[9] This fibroin membrane, with platinum thin-film electrodes on top, was completely biodegradable within 10 days in the presence of a protease from *Streptomyces griseus*, type XIV, without causing any cytotoxic reactions. However, the fabrication of the platinum electrodes by means of the physical vapor deposition process requires a clean room and high vacuum ($<10^{-6}$ mbar) conditions, in which the latter put the water-containing fibroin membrane under stress. As a consequence, the lifetime of the platinum thin-film electrodes is limited. To circumvent these drawbacks, thick-film technology for electrode deposition, particularly screen-printing, enables the fabrication of a screen-printed biosensor based on carbon electrodes on a biodegradable fibroin substrate.^[37] The biosensor performance was studied regarding curing parameters, applied working electrode potential, and shelf life. The sensors demonstrated that thick-film technology represents a promising strategy for fabricating flexible and biocompatible biosensors. In contrast, the utilized silicone-containing carbon paste as well as the encapsulation material (Ecoflex) would not be fully biodegradable under physiological conditions.^[38]

Therefore, the hereafter reported experiments were intended to address two different issues: application of 1) a water-based carbon paste for fabrication of screen-printed electrodes on biodegradable membranes of fibroin and PLA, and of 2) fibroin, PLA, and wound adhesive as alternative encapsulation materials for replacement of the Ecoflex encapsulation layer. For the screen-printed carbon electrodes, the curing parameters were examined with regard to the glucose biosensor functionality (with immobilized enzyme glucose oxidase) in the glucose concentration range from 0.5 to 10 mM (via chronoamperometry). To study the capability of fibroin, PLA, and wound adhesive as an alternative encapsulation material, swelling tests in aqueous solutions as well as chronoamperometric experiments (in 0.5 to 10 mM H_2O_2 -containing solutions) of fully covered chip surfaces were performed, to exclude any leakage current through these layers.

2. Experimental Section

2.1. Materials

Triol (99.5%), ethanol (99%), glucose monohydrate (99%), and glucose oxidase (GO_x) from *Aspergillus niger* (E.C. 1.4.4.), bovine

serum albumin (96%), disodium hydrogen phosphate dihydrate (analytical grade), and sodium dihydrogen phosphate monohydrate (analytical grade) were purchased from Sigma-Aldrich (St. Louis, USA). Ecoflex 00-30 was obtained from KauPo Plankenhorn e.K. (Spaichingen, Germany). Directly before use, the two components of Ecoflex were mixed in a 1:1 ratio and degassed in vacuum until all bubbles disappeared. Hydrogen peroxide (35%) was acquired from MC Industrial Chemicals (Philadelphia, USA). Glutaraldehyde (25%) was purchased from Acros Organics (Geel, Belgium). The silk fibroin aqueous solution was obtained using PureSilk technology (Fibrothelium GmbH, Aachen, Germany) enabling medical-grade quality on an industrial scale for a broad range of concentrations. Briefly, fibroin was separated from sericin by degumming it in a hot alkali solution before dissolving it in a proprietary nontoxic solvent system based on Ajisawa's reagent. The dissolved fibroin was fully dialyzed against DI water within 8 h using tailored extraction processing and stored in a freezer at -20°C . The conductive carbon paste Custom Ink/CMC 12 072 021 was purchased from Cambridge Graphene Ltd. (Gloucestershire, England) and stored at 4°C in the refrigerator. The silver conducting ink (article number: 530042) was bought from Ferro GmbH (Frankfurt am Main, Germany).

2.2. Preparation of the Fibroin Membrane

The fibroin membrane was prepared under cleanroom conditions at 21°C . The formulation of the fibroin membrane used as substrate for the carbon electrodes consisted of 2 vol.-eq. of an 8 wt% solution of PureSilk, 1 vol.-eq. of 50 vol% ethanol solution, and 1 vol.-eq. of 3 vol% triol solution. 10 mL of the final mixture was casted onto the flat surface of a petri dish and dried for 2 days. The dried membrane was then carefully detached from the surface. The resulting membrane had a diameter of 9 cm, of which 0.5 cm is cut off at the edge to obtain a flexible membrane. Further details on the preparation of fibroin membranes can be found elsewhere.^[9,37] The samples for the swelling tests were prepared using the same procedure (with the formulation adjusted accordingly), as described in Section 2.6.

2.3. Fabrication of the Biocompatible Biosensor via Thick-Film Technology

The carbon working electrodes were screen-printed onto fibroin and PLA substrates, respectively, with a semiautomatic screen-printing machine from Hary Manufacturing Inc. (Lebanon, USA) using a $40\ \mu\text{m}$ thick template, as shown in **Figure 1**, left.

The PLA foil was treated before with an oxygen plasma at 100 W for 60 s (Diener Electronic GmbH + Co. KG, Ebhausen, Germany) to achieve a homogenous spread of the carbon paste. To solidify the carbon paste, the screen-printed carbon electrodes on fibroin were cured either at room temperature for 18 h, at 50°C for 24 h, at 80°C for 24 h, at 100°C for 20 min, or at 160°C for 1 h, **Figure 1** (middle). Due to the different melting and softening points of the two substrates, the curing temperatures of the carbon electrodes on the PLA substrate were different: they were cured at room temperature for 18 h, at 50°C

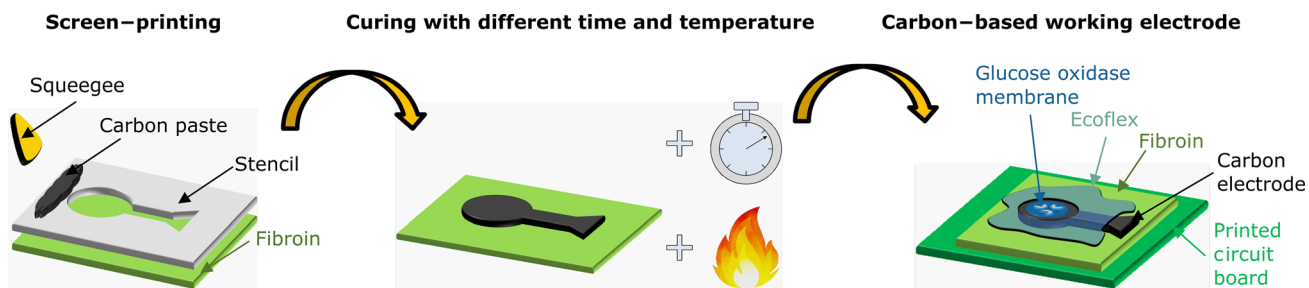


Figure 1. Schematic of the manufacturing process of a carbon-based working electrode on a fibroin substrate. The process starts with screen-printing of the carbon paste onto the fibroin substrate (left), followed by a curing step of the carbon paste with different curing times and curing temperatures (middle). The final layout of the working electrode, consisting of a printed circuit board with a carbon electrode modified by glucose oxidase on fibroin and encapsulated with Ecoflex, is shown on the right.

for 24 h, at 65 °C for 24 h, at 80 °C for 30 min, and at 100 °C for 10 min.

The flexibility of the carbon electrode on the fibroin substrate decreased with increasing temperature, but even at 160 °C for 1 h, the electrode could be bent to the point where the corners of the substrate touched, see **Figure 2a**. In contrast, the flexibility of the carbon electrodes on PLA was only slightly affected by the curing temperatures. As an example, **Figure 2b** shows a carbon electrode on PLA, cured at 65 °C for 24 h. For subsequent electrochemical sensor characterization, the as-prepared electrodes were separated and fixed to a printed circuit board using biocompatible Ecoflex as an adhesive layer. After drying, electrical

contact was made between the carbon electrode and the track of the circuit board via conductive silver paint and aluminum foil. The entire electrode was encapsulated by the addition of a previously casted Ecoflex film with a 5 mm hole (opened for enzyme immobilization and contact to the analyte), also utilizing Ecoflex as the adhesive layer. The processed carbon electrode was exposed to an oxygen plasma at 100 W for 60 s and afterward modified with glucose oxidase. For this, a solution consisting of a 1–2–2 mixture of glucose oxidase ($5 \text{ U } \mu\text{L}^{-1}$), bovine serum albumin, and glutaraldehyde/triol was drop-coated onto the free surface of the carbon electrode, see also in the study by Molinnus et al.^[39]

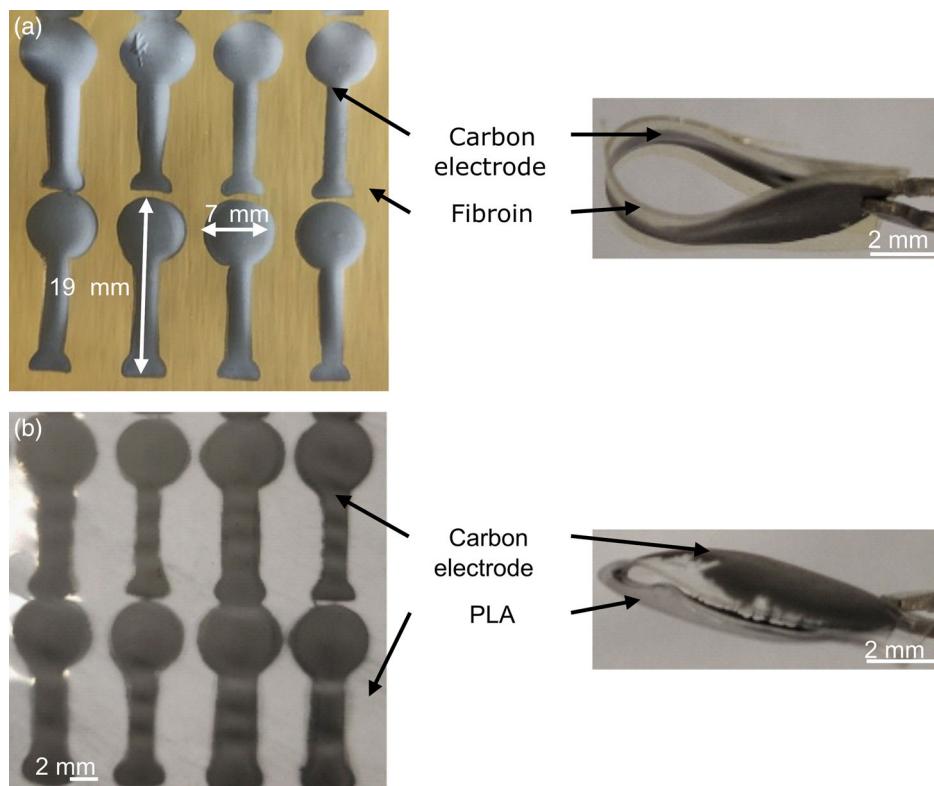


Figure 2. a) Photo of the screen-printed and cured carbon electrodes on fibroin at 160 °C for 1 h on a flat surface (left) and in the bent state (right). b) Photo of the screen-printed and cured carbon electrodes on PLA at 65 °C for 24 h on a flat surface (left) and in the bent state (right).

2.4. Fabrication of the Fully Encapsulated Carbon Electrodes for Leakage Current Experiments

To investigate the encapsulation functionality of fibroin, Ecoflex, and PLA, the carbon electrodes were screen-printed as described previously. The electrodes on fibroin were cured at 160 °C for 1 h, while those on PLA were cured at 65 °C for 24 h. These curing profiles were chosen as they resulted in the best sensor performance for glucose measurements, as described in Section 3.2. The carbon electrode was completely covered with the material under investigation. Ecoflex encapsulation was applied as previously described. A PLA film was adhered with “Trueglue wound adhesive” (Pflege Discount Gelnhausen GmbH, Gelnhausen, Germany). Fibroin encapsulation was applied with water and pressure. Both the fibroin used as encapsulation and as substrate material were moistened with water. The materials were placed between two soft laboratory cloths, loaded with 1 kg and dried, to achieve the adhesion between the fibroin encapsulation and the carbon electrode.

2.5. Measurement Protocol for the Chronoamperometric Characterizations

The chronoamperometric experiments were performed in a three-electrode setup consisting of a conventional Ag/AgCl reference electrode (Deutsche Metrohm GmbH & Co. KG, Filderstadt, Germany), a platinum wire as counter electrode (MaTeck, Jülich, Germany) and the functionalized thick-film carbon electrode as working electrode. All electrodes were connected to a potentiostat (PalmSens3, Palm Instruments BV, GA Houten, The Netherlands) and controlled by the software PSTrace. Measurements were performed at 21 °C in a stirred phosphate buffer solution (PBS) at pH 7.4, which corresponds to the pH of human blood. The measurement principle of the biosensor is based on the conversion of glucose into D-glucono-1,5-lactone and hydrogen peroxide (H_2O_2) in the presence of the enzyme glucose oxidase and oxygen. H_2O_2 is oxidized on the surface of the carbon working electrode and the resulting current is recorded over time. For amperometric measurements, glucose concentrations ranging from 0.5 to 10 mM were diluted using a 250 mM glucose stock solution. Each glucose concentration was measured for 10 min with a potential of 1.2 V applied to the carbon working electrode versus the Ag/AgCl reference electrode.

The encapsulation studies were performed using H_2O_2 as an analyte because the entire electrode was encapsulated and no

glucose oxidase membrane could be applied. Here, different H_2O_2 concentrations (0.5–10 mM) were prepared from a 250 mM stock solution.

2.6. Measurement Protocol for the Swelling Experiments

The fibroin samples were casted according to the protocol in Section 2.2; however, the composition of the formulation was varied. For this purpose, the total volume of 10 mL to be poured into the Petri dish was kept constant. The PLA film was used directly for the experiment without any further treatment. The Ecoflex sample was poured onto a flat surface to form a film of approximately 2 mm thickness. The swelling experiment sequence is shown in Figure 3. Each sample was first weighed in the dry state and then submerged in PBS, pH 7.4, in a closed vessel for 24 h. The sample was removed from the vessel, supernatant drops of PBS were carefully removed with an absorbent laboratory cloth, and the sample was weighed in the wet state, too. The wet sample was dried on the laboratory bench for 24 h and weighed again in the dry state.

3. Results and Discussion

3.1. Scanning Electron Microscopy of the Carbon Working Electrode, Screen-Printed on Fibroin or Poly lactide

The thick-film carbon electrodes, screen-printed onto the biodegradable substrates fibroin and PLA, and cured with the different temperature profiles, were characterized by scanning electron microscopy (SEM, JEOL JSM-7800F, Freising, Germany) with an applied acceleration voltage of 5.0 kV. The SEM images in Figure 4 address a cross-sectional view of the carbon working electrode, screen-printed on fibroin (Figure 4a) and on PLA (Figure 4g), respectively, as well as a top view to the middle of the sensing area for fibroin (Figure 4b–f) and PLA (Figure 4h–l), utilizing different curing parameters.

For both substrate materials, the top-view images of the carbon working electrode show a homogeneous, uniform 3D structure with overlapping carbon flakes with 1.5 μm in size, regardless of the curing profile applied. The fibroin or PLA substrate layer can be easily distinguished from the carbon layer in the cross-sectional view. Also here, no obvious effect on the carbon layer morphology can be observed.

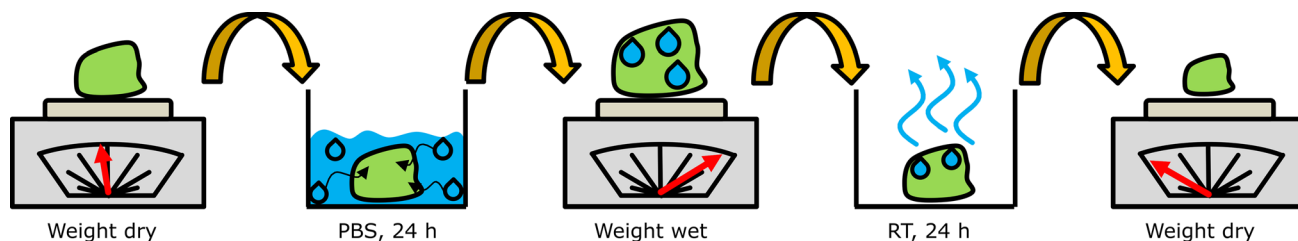


Figure 3. Swelling test sequence. The sample is first weighed in the dry state, submerged in PBS (pH 7.4) for 24 h, then weighed in the wet state, and weighed again after 24 h of drying at room conditions.

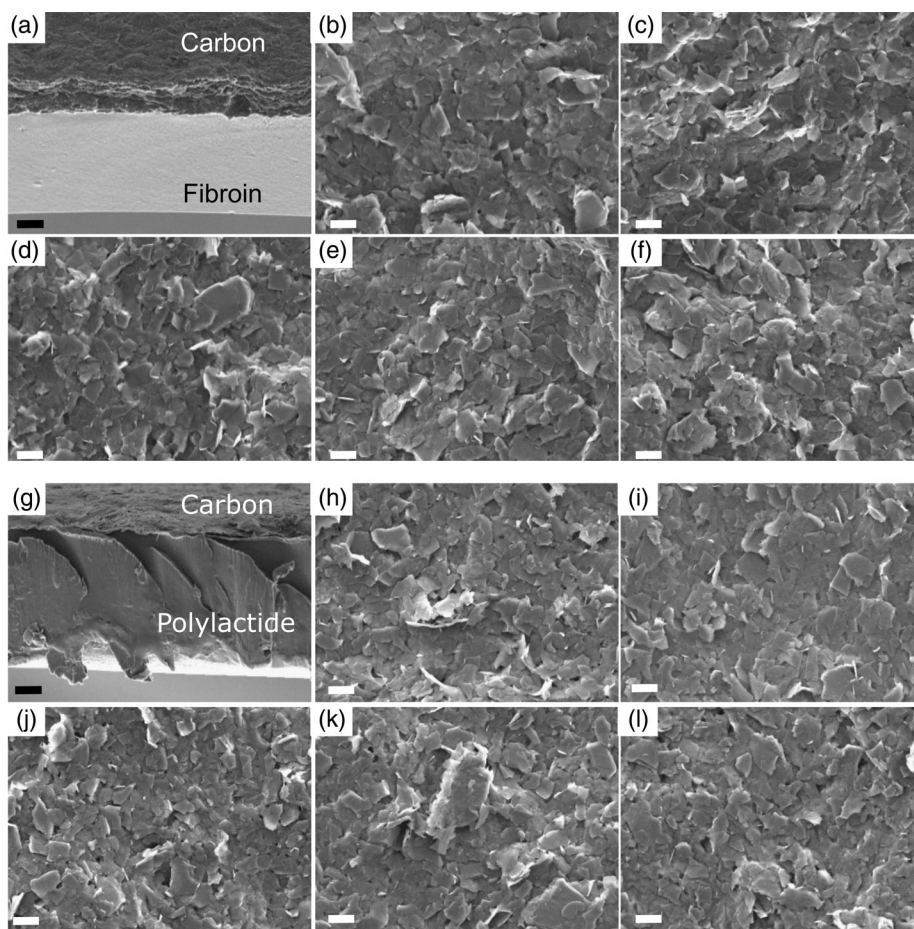


Figure 4. SEM images of the carbon working electrodes, screen-printed on fibroin with a cross-sectional view through the sensing area of the electrode a), and top view of the sensing area b–f). SEM images of carbon working electrodes, screen-printed on polylactide with a cross-sectional view through the sensing area of the electrode g) and top view of the sensing area h–l). The white scale bars indicate 2 μm , and the black scale bars 10 μm . Curing parameters: (a), (f) 160 $^{\circ}\text{C}/1\text{ h}$; (b) room temperature/18 h; (c) 50 $^{\circ}\text{C}/24\text{ h}$; (d) 80 $^{\circ}\text{C}/24\text{ h}$; (e) 100 $^{\circ}\text{C}/20\text{ min}$; (g,i) 65 $^{\circ}\text{C}/24\text{ h}$; (h) room temperature/18 h; (i) 50 $^{\circ}\text{C}/24\text{ h}$; (k) 80 $^{\circ}\text{C}/30\text{ min}$; (l) 100 $^{\circ}\text{C}/10\text{ min}$.

3.2. Influence of Curing Parameters for a Biodegradable Carbon Paste on Glucose Biosensor Performance

A series of chronoamperometric glucose measurements was performed to determine the effect of selected curing profiles on the sensitivity of the two different biosensors with fibroin and PLA as substrate material. The experiments were performed in PBS, pH 7.4, with a working potential of 1.2 V applied to the carbon electrode versus the Ag/AgCl reference electrode. The resulting calibration curves of the different applied curing profiles (room temperature (RT) for 18 h (black), 50 $^{\circ}\text{C}$ for 24 h (red), 80 $^{\circ}\text{C}$ for 24 h (green), 100 $^{\circ}\text{C}$ for 20 min (blue), and 160 $^{\circ}\text{C}/1\text{ h}$ (cyan)) utilizing fibroin as substrate material are shown in **Figure 5a**.

As expected, the measured current increases with increasing glucose concentration due to the enzymatic reaction at the carbon electrode surface (generation of H_2O_2 that is oxidized at the applied working potential). All carbon electrodes respond immediately to the addition of glucose, but the higher the curing temperature of the carbon electrode, the more pronounced the steps become (data not shown). The highest signal change

between 0.5 and 10 mM glucose was obtained for a GO_x -modified carbon electrode on fibroin cured at 160 $^{\circ}\text{C}$ for 1 h (cyan). The current generated at 10 mM was about 690 nA mm^{-2} , which is almost six times higher than for a carbon electrode cured at 100 $^{\circ}\text{C}/20\text{ min}$ (blue). The mean sensitivities, calculated by a linear fit between 0 and 3 mM glucose, also indicate a similar behavior (see **Figure 5b**). The 160 $^{\circ}\text{C}/1\text{ h}$ profile (cyan) with a sensitivity of $142.4 \pm 11\text{ nA mm}^{-2}\text{ mM}^{-1}$ is almost 10 times higher than the 100 $^{\circ}\text{C}/20\text{ min}$ profile (blue) with $14.1 \pm 0.9\text{ nA mm}^{-2}\text{ mM}^{-1}$. However, as shown in **Table 1**, the absolute standard deviation of the mean glucose sensitivity also raises with increasing curing temperature.

The carbon electrodes printed on PLA were studied under the same conditions as for the carbon electrodes on fibroin. **Figure 6a** shows the resulting current change of the biosensors to variations of the glucose concentration between 0.5 and 10 mM for differently cured carbon electrodes including a linear fit between 0 and 3 mM glucose. In contrast to the fibroin-based biosensors, this type based on PLA gave the best sensor performance with a mean glucose sensitivity of $71.1 \pm 4.7\text{ nA mm}^{-2}\text{ mM}^{-1}$

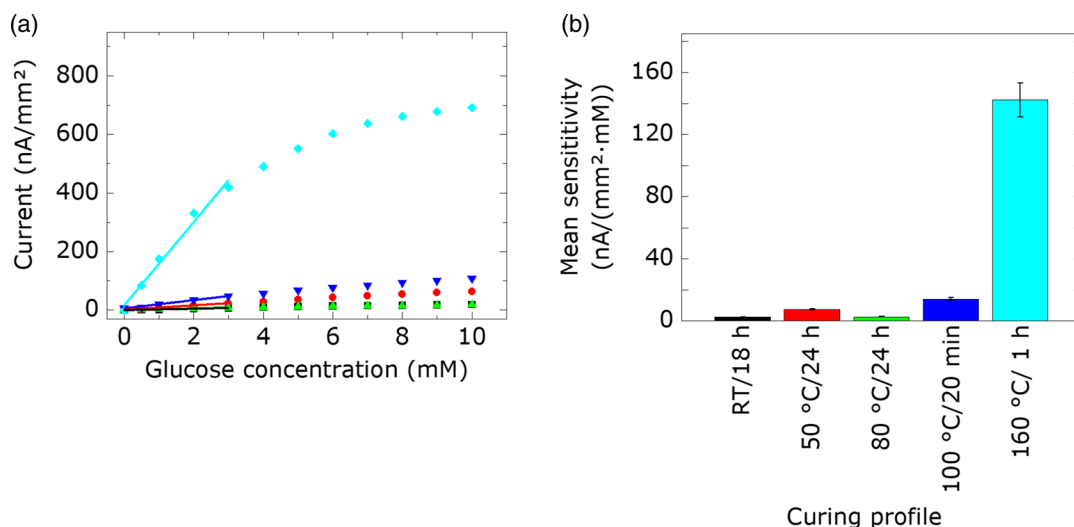


Figure 5. a) Exemplary amperometric response of the thick-film glucose biosensor printed on fibroin with immobilized GO_x , measured in PBS (pH 7.4) versus Ag/AgCl (1.2 V) for different glucose concentrations (0.5–10 mM). The carbon electrode on fibroin was cured with different curing profiles: room temperature (RT) for 18 h (black), 50 °C for 24 h (red), 80 °C for 24 h (green), 100 °C for 20 min (blue), and 160 °C/1 h (cyan). b) Corresponding mean sensitivities (0–3 mM, $n = 6$ sensors) evaluated from (a). All measurement curves in (a) were normalized to their initial starting value in PBS, GO_x : glucose oxidase.

Table 1. Mean glucose sensitivity (0–3 mM) and standard deviation for screen-printed carbon electrodes on fibroin and PLA, respectively ($n = 6$ sensors).

| Substrate material | Curing profile | Mean sensitivity [$\text{nA mm}^{-2} \text{mM}^{-1}$] |
|--------------------|-----------------------|---|
| Fibroin | Room temperature/18 h | 2.4 ± 0.3 |
| | 50 °C/24 h | 7.5 ± 0.4 |
| | 80 °C/24 h | 2.6 ± 0.2 |
| | 100 °C/20 min | 14.1 ± 0.9 |
| | 160 °C/1 h | 142.4 ± 11 |
| PLA | Room temperature/18 h | 1.2 ± 0.3 |
| | 50 °C/24 h | 40.4 ± 3.2 |
| | 65 °C/24 h | 71.1 ± 4.7 |
| | 80 °C/30 min | 32.8 ± 5.4 |
| | 100 °C/10 min | 7.2 ± 0.6 |

for the electrode, cured at 65 °C for 24 h (green, Figure 6b). The maximum achievable sensitivity is consequently half the sensitivity of the biosensors on the fibroin substrate. Unlike, biosensors with carbon working electrode screen-printed on PLA are less brittle in comparison to carbon electrodes on fibroin substrate.

In summary, carbon electrodes screen-printed on fibroin need a high temperature but short curing profile (160 °C/1 h, cyan) to achieve high sensitivities in amperometric measurements. However, the layers become brittle due to the manufacturing process applying the high temperature. In contrast, for carbon electrodes screen-printed on PLA, a moderate curing profile (65 °C/24 h, green) was favorable. Table 1 overviews the mean glucose sensitivities for all combinations of investigated substrate materials and curing profiles.

3.3. Swelling Behavior of Tested Encapsulation Materials Fibroin, Poly lactide, and Ecoflex

Ecoflex is a cross-linked polybutylene adipate terephthalate, which can be biodegraded in industrial composting facilities within a few weeks.^[40] At the same time, only a little information can be found in the literature about the biodegradation of Ecoflex under more physiological conditions; Scaffaro et al. discussed, for example, the possibility of hydrolysis and enzymatic degradation of Ecoflex.^[41] In contrast, the biodegradability of fibroin can be influenced by manipulating the β -sheet fraction in the semi-crystalline polymer.^[42,43] The β -sheet content influences not only the velocity of biodegradation, but also other properties such as water solubility, tensile strength, and flexibility.^[44] Several methods are discussed to influence the β -sheet fraction, such as, by exposing the sample to water, ethanol, or methanol vapor.^[45–47] These cause crystallization within the fibroin sample, resulting in a physical cross-linking. The properties of PLA can also be adjusted by its crystal content, however, this is primarily influenced by the ratio of the monomers.^[48]

The encapsulation of the carbon electrodes for amperometric measurements serves to define the sensitive surface area of the working electrode and to isolate and protect the conductive path and electrical connections. Therefore, ideally, the encapsulation shall not be permeable for analyte molecules. To replace Ecoflex by an alternative material whose biodegradation mechanism can be controlled, a series of swelling experiments was conducted with different fibroin formulations (different glycerol and ethanol concentrations), PLA, and polyimide (as a not biodegradable encapsulation material in comparison). Figure 7 shows the change of weight of the examined materials with blue bars (wet state) representing the difference between the original weight and the wet weight, and red bars (dried state)

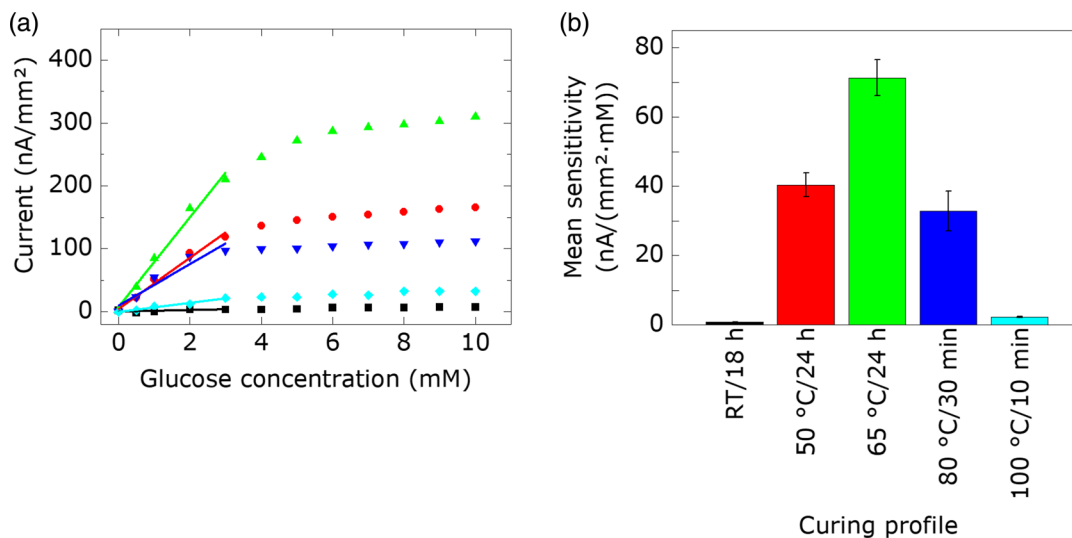


Figure 6. a) Exemplary amperometric response of the thick-film glucose biosensor screen-printed on PLA with immobilized GO_x, measured in PBS (pH 7.4) versus Ag/AgCl (1.2 V) for different glucose concentrations (0.5–10 mM). The carbon electrode on PLA has been cured with different curing profiles: room temperature (RT) for 18 h (black), 50 °C for 24 h (red), 65 °C for 24 h (green), 80 °C for 30 min (blue), and 100 °C/10 min (cyan). b) Corresponding mean sensitivities (0–3 mM, $n = 6$ sensors). All measurement curves in (a) were normalized to their initial starting value in PBS, GO_x: glucose oxidase.

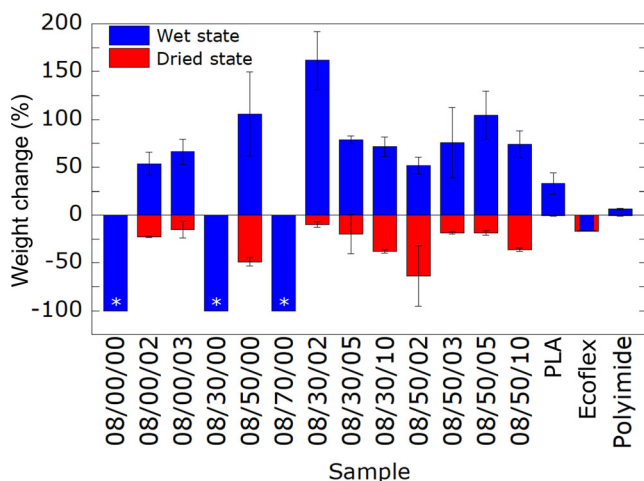


Figure 7. Weight change in relation to the original sample weight of various fibroin formulations, PLA, Ecoflex, and polyimide after 24 h swelling in PBS, pH 7.4 (wet state, blue), and subsequent 24 h drying (dried state, red). The asterisk indicates specimens that lost dimensional stability during swelling. Nomenclature: e.g., 08/30/02 = 8 wt% PureSilk (fibroin) solution, 30 vol% ethanol solution, and 2 vol% triol solution were mixed in a 2:1:1 ratio; $n = 3$ sensors tested for each composition.

corresponding to the weight difference after drying again for 24 h; see also Section 2.6. The fibroin samples were named according to their formulation: the fibroin formulation consists of two parts fibroin, one part ethanol and one part triol solution. The numbers given in the diagram represent the percentages by weight (in the case of fibroin solution) or by volume of the other solutions used. For example, the fibroin recipe 08/50/03 consists of 8 wt% fibroin solution with one part of 50 vol% ethanol solution and one part of 3 vol% triol solution.

The swelling experiments demonstrated that, depending on the selected recipe, the degree of swelling and also the water solubility of the membrane can be controlled. Pure fibroin (08/00/00) without additives is water-soluble as described in the literature.^[49] The asterisks, as well as the missing error bars for the recipes 08/00/00, 08/30/00, and 08/70/00 indicated that the membranes dissolved in water and lost their dimensional stability. The addition of 50 vol% ethanol resulted in a more preferential, insoluble fibroin membrane (08/50/00). Triol, which was added to the fibroin solution, primarily acts as a plasticizer, also resulting in water-insoluble membranes (e.g., 08/00/03). Presumably, the hydroxide groups of the triol react with the functional groups of the fibroin, cross-linking them. In contrast, the combination of triol and ethanol in the fibroin membrane formulation did not result in lower weight changes. Rather, a sample such as 08/50/03 absorbed more PBS than the corresponding sample without ethanol (08/00/03). All fibroin formulations absorbed at least 50% of their own weight (see blue bars).

In contrast, PLA absorbed only about 30% of its own weight; it was additionally observed that the penetration with PBS was more slowly compared to that of the fibroin samples. Unlike the fibroin samples, the PLA sample showed almost no loss of mass after drying (red bars), which was also reflected in the consistent flexibility of the sample. Presumably, short fibroin chains, which often act as plasticizers in polymeric materials, were leaking out when the fibroin samples were swelling.^[50] All tested fibroin membranes were hard and brittle after drying them again. Interestingly, the Ecoflex samples became even lighter during “swelling.” This could be due to the hydrolysis of Ecoflex or the loss of short polymer chains during the swelling experiment.^[41] The nonpolar, nonbiodegradable encapsulation material polyimide gained the least amount of weight (less than 10%) and also had the least weight loss (less than 1%) after drying again.

In summary, the different fibroin membrane formulations exhibited a distinct influence on the swelling behavior of the membranes. However, all fibroin membranes increased at least 50% of their own weight, which was significantly larger than for the commercial PLA film studied, which prevents water penetration more obviously. The not biodegradable polyimide film exhibits high stability. It gained the least weight during swelling and also had the least weight loss after subsequent drying.

3.4. Electrochemical Investigation of a Fully Encapsulated Carbon-Based Electrode

In addition to the swelling experiments, amperometric studies were applied to record the (possible) leakage current through the encapsulation layers, resulting from varying H_2O_2 concentrations in the analyte solution. For this purpose, the screen-printed carbon electrode was fully encapsulated with the material under investigation. A material is assumed to be suitable as an encapsulation if the working electrode (at a certain applied potential versus the Ag/AgCl reference electrode) does not detect the addition of H_2O_2 to the analyte. Four different encapsulation materials were investigated: Ecoflex, PLA, fibroin, and wound adhesive. Ecoflex is a two-component mixture that hardens over time and was drop-casted onto the electrode's surface. Fibroin attachment to the electrode was achieved by

moistening with distilled water and drying under pressure, see Section 2.4. In case of PLA, a biodegradable wound adhesive, which is also used in medical surgeries, was selected to fix the PLA film onto the carbon electrode. Additionally, the wound adhesive alone was checked for its insulating properties, therefore further electrodes were also coated with it and investigated. A "normal" sensor with a defined exposed electrode area to the analyte (hole with 5 mm diameter in the Ecoflex passivation) served as a reference in all experiments to validate the operational capability of the carbon electrode toward H_2O_2 .

Figure 8 shows the dynamic amperometric response to H_2O_2 titrations between 0.5 and 10 mM for fully encapsulated carbon-based electrodes, screen-printed on fibroin (Figure 8a) or PLA (Figure 8b), carrying different encapsulation materials (red, blue, green, cyan curves). In addition, the not completely covered carbon electrode is depicted as black curve.

In Figure 8a,b, the concentration dependence of the "reference" carbon working electrode toward varying H_2O_2 concentrations (black) is depicted from 0.5 to 10 mM, which resulted in clear concentrations steps and a comparable behavior for both types of electrode (fibroin and PLA substrate). For the fully encapsulated sensors, the electrodes with wound adhesive encapsulation (green) also reacted to a certain extent to the addition of H_2O_2 for both substrates, although this appeared to be more pronounced for the carbon electrodes on fibroin than those on PLA. This behavior is consistent with the results of sensitivity measurements for the different curing parameters (see Section 3.2),

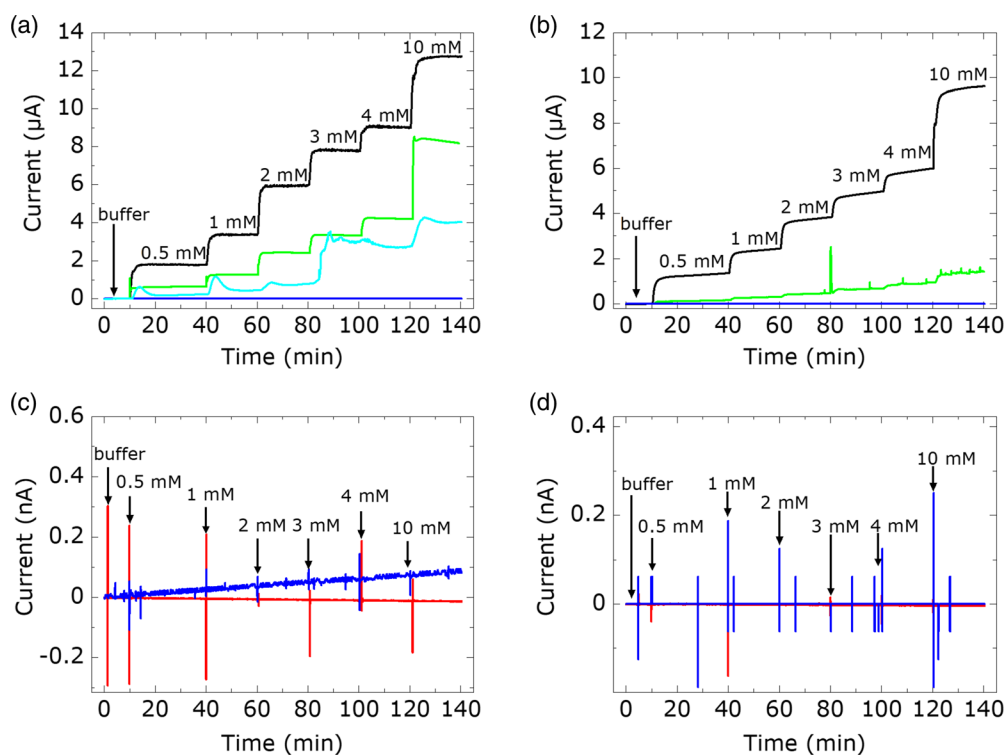


Figure 8. Dynamic amperometric response of the sensor chip to different H_2O_2 titrations (0.5–10 mM) at 1.2 V versus the Ag/AgCl reference electrode of a fully encapsulated carbon working electrode, screen-printed on a) fibroin and cured at 160 °C for 1 h, and b) PLA, cured at 65 °C for 24 h. The carbon working electrodes were encapsulated in Ecoflex (red), wound glue (green), wound glue together with PLA (blue), and for (a) in fibroin (cyan), too. Black curves: not completely covered carbon electrode as a "reference" for H_2O_2 determination. c,d): magnified view of current measurements in (a) and (b) for wound glue together with PLA (blue) and Ecoflex (red).

where the carbon electrodes on the fibroin substrate gave higher signal changes. The carbon electrodes encapsulated with fibroin also showed some response to H₂O₂ addition (cyan). However, it is noticeable that the signal changes had a slight delay and no clear concentration dependency was found, indicating that the fibroin at least gave some barrier functionality. One explanation might be due to the longer diffusion path of the analyte molecules through the swollen membrane.^[42] Ecoflex and the material combination of wound adhesive and PLA prevented a sensory reaction to the addition of H₂O₂. Especially, the findings for PLA emphasize the results of swelling tests in Section 3.3.

The measurement of the leakage current of fully encapsulated carbon electrodes on fibroin or PLA substrate, respectively, showed that the combination of the biodegradable materials PLA and wound adhesive resulted in a promising alternative to the Ecoflex encapsulation. Like Ecoflex, PLA together with wound adhesive prevented the oxidation of H₂O₂ at the carbon electrode surface for a period of 140 min. In the next step, the long-term stability of the PLA and wound adhesive combination should be investigated in more detail. In contrast, a carbon electrode with a fibroin encapsulation showed only insufficient barrier properties. The recorded leakage current, due to the oxidation of H₂O₂ at the carbon electrode surface, appeared with a time delay compared to the “reference” carbon working electrode. Adjusting the properties of the fibroin membrane (e.g., increasing the crystallinity) and increasing the encapsulation layer thickness could further extend the barrier functionality. However, wound adhesive encapsulation alone did not provide barrier effects, the recorded leakage current appeared immediately.

4. Conclusions

Silicone-free carbon electrodes on fibroin and polylactide substrates were prepared by thick-film technology and solidified with different curing profiles ranging from 24 h at room temperature to 1 h at 160 °C. The influence of these parameters on the morphology of the carbon electrodes and the electrochemical properties of an exemplary glucose oxidase membrane-modified biosensor was determined. Biomedically relevant glucose concentrations between 0.5 and 10 mM glucose in PBS, pH 7.4, were analyzed by chronoamperometry. The carbon electrode with modified glucose oxidase membrane, screen-printed on a flexible fibroin substrate, achieved the highest sensitivity (142.4 ± 11 nA/(mm² mM)) utilizing a short curing time (1 h) combined with a high curing temperature (160 °C). The carbon electrode-based biosensor on PLA, in contrast, obtained the optimal results at a curing profile of 65 °C for 24 h, reaching a sensitivity of 71.1 ± 4.7 nA/(mm² mM). In both cases, the silicone-free carbon electrodes and their biodegradable substrates remained flexible after curing.

Swelling studies (for PBS) and chronoamperometric measurements of possible diffusion of H₂O₂ molecules through fully encapsulated carbon electrodes on fibroin and PLA should prove the encapsulation layer's behavior. The materials Ecoflex, fibroin, and PLA together with wound adhesive were investigated for their encapsulation capability. Best properties were obtained for an encapsulation layer of Ecoflex, or PLA in combination with

wound adhesive. These materials were able to prevent the diffusion of H₂O₂ from the analyte to the carbon electrode surface during a measurement period of about 140 min.

This work highlights the versatility of fibroin for future biomedical applications. The wide range of modification options for fibroin enables the adjustment of properties, like swelling behavior, transparency, mechanical properties, or the rate of biodegradation.^[43,44] In this way, fibroin can be used as a mechanically resistant substrate for screen-printed carbon electrodes or as a swellable membrane for exemplary drug-delivery devices.^[37,45,46] Fibroin can adopt a variety of morphologies such as sponges, fibers, or gels.^[47–49] Thus, fibroin could even be tried as an alternative to the biomedical wound adhesive.^[47] The outstanding properties of fibroin, especially its intrinsic biocompatibility and biodegradability, make it an excellent material for implantable sensors in future or transient medical devices. In this scenario, fibroin could serve as a time-controlled degradable substrate for a fully implantable biosensor for in-vivo applications, e.g., postoperative monitoring. This way, the sensor's biodegradability would eliminate the need for a second surgery to remove the biosensor at the end of its service life.

Acknowledgements

The authors thank D. Rolka for assistance with the SEM images, G. Celep for supporting the swelling experiments, and D. Molinnus for valuable discussions.

Open Access funding enabled and organized by Projekt DEAL.

Conflict of Interest

The authors declare no conflict of interest.

Data Availability Statement

The data that support the findings of this study are available from the corresponding author upon reasonable request.

Keywords

amperometric biosensors, biocompatible, biodegradable, encapsulation materials, fibroin

Received: February 6, 2023

Revised: April 3, 2023

Published online: May 31, 2023

- [1] Y. Li, W. Chen, L. Lu, *ACS Appl. Bio Mater.* **2021**, *4*, 122.
- [2] L. Wang, Z. Lou, K. Jiang, G. Shen, *Adv. Intell. Syst.* **2019**, *1*, 1900040.
- [3] J. Li, Y. Long, F. Yang, X. Wang, *Curr. Opin. Solid State Mater. Sci.* **2020**, *24*, 100806.
- [4] W. Noura, R. Haddad, H. Barhoumi, A. Maaref, J. Bausells, F. Bessueille, D. Léonard, N. Jaffrezic-Renault, A. Errachid, *Sens. Lett.* **2022**, *7*, 113728.
- [5] E. González-Fernández, M. Staderini, J. R. K. Marland, M. E. Gray, A. Uçar, C. Dunare, E. O. Blair, P. Sullivan, A. Tsiamis, S. N. Greenhalgh, R. Gregson, R. E. Clutton, S. Smith, J. G. Terry,

- D. J. Argyle, A. J. Walton, A. R. Mount, M. Bradley, A. F. Murray, *Biosens. Bioelectron.* **2022**, *197*, 113728.
- [6] J. Tan, *Int. J. Electrochem. Sci.* **2022**, *17*, 22015.
- [7] S. K. Mahadeva, J. Nayak, J. Kim, *Proc. SPIE* **2011**, *7980*, 114.
- [8] J. Njagi, M. M. Chernov, J. C. Leiter, S. Andreev, *Anal. Chem.* **2010**, *82*, 989.
- [9] D. Molinnus, A. Drinic, H. Iken, N. Kröger, M. Zinser, R. Smeets, M. Köpf, A. Kopp, M. J. Schöning, *Biosens. Bioelectron.* **2021**, *183*, 113204.
- [10] D. Zhang, X. Wu, J. Chen, K. Lin, *Bioact. Mater.* **2018**, *3*, 129.
- [11] J. E. Oliveira, L. H. C. Mattoso, E. S. Madeiros, V. Zucolotto, *Biosensors* **2012**, *2*, 70.
- [12] J.-Z. Wang, M.-L. You, Z.-Q. Ding, W.-B. Ye, *Mater. Sci. Eng., C* **2019**, *97*, 1021.
- [13] M. Teodorescu, M. Bercea, S. Morariu, *Biotechnol. Adv.* **2019**, *37*, 109.
- [14] X. Sun, W. Zhong, Z. Zhang, H. Liao, C. Zhang, *J. Mater. Sci.* **2022**, *57*, 12511.
- [15] S. Pradhan, V. K. Yadavalli, *ACS Appl. Electron.* **2021**, *3*, 21.
- [16] S. Střiteský, A. Marková, J. Viteček, E. Šafaříková, M. Hrabal, L. Kubáč, L. Kubala, M. Weiter, M. Vala, *J. Biomed. Mater. Res. A* **2018**, *106*, 1121.
- [17] C. G. Sanz, M. Onea, A. Aldea, M. M. Barsan, *Talanta* **2022**, *241*, 123255.
- [18] S. B. Qasim, M. S. Zafar, S. Najeed, Z. Khurshid, A. H. Shah, S. Husain, I. U. Rehman, *Int. J. Mol. Sci.* **2018**, *19*, 407.
- [19] S. Tiwari, P. Bahadur, *Int. J. Biol. Macromol.* **2019**, *121*, 556.
- [20] K. Ren, Y. Chen, C. Huang, R. Chen, Z. Wang, J. Wei, *J. Mater.* **2019**, *7*, 5704.
- [21] D. B. Cybyk, B. M. Reinsch, K. F. Presley, R. M. Schweller, A. Tedeschi, T. Burns, F. J. Chaparro, J. T. Ly, M. J. Dalton, M. Lozano, T. A. Grusenmeyer, J. J. Lannutti, *Med. Devices Sens.* **2021**, *4*, 10149.
- [22] R. Gifford, J. J. Kehoe, S. L. Barnes, B. A. Kornilayev, M. A. Alterman, G. S. Wilson, *Biomaterials* **2006**, *27*, 2587.
- [23] D. Chan, J.-C. Chien, E. Axpe, L. Blankemeier, S. W. Baker, S. Swaminathan, V. A. Piunova, D. Y. Zubarev, C. L. Maikawa, A. K. Grosskopf, J. L. Mann, H. T. Soh, E. A. Appel, *Adv. Mater.* **2022**, *34*, 219764.
- [24] C. Lee, S. Kim, Y.-H. Cho, *Adv. Sustainable Syst.* **2022**, *6*, 20002116.
- [25] F. Chen, D. Porter, F. Vollrath, *Acta Biomater.* **2012**, *8*, 2620.
- [26] D.-L. Wen, D.-H. Sun, P. Huang, W. Huang, M. Su, Y. Wang, M.-D. Han, B. Kim, J. Brugger, H.-X. Zhang, X.-S. Zhang, *Microsyst. Nanoeng.* **2021**, *7*, 35.
- [27] D.-L. Wen, Y.-X. Pang, P. Huang, Y.-L. Wang, X.-R. Zhang, H.-T. Deng, X.-S. Zhang, *Adv. Fiber Mater.* **2022**, *4*, 873.
- [28] I. P. Moreira, C. Esteves, S. I. Palma, E. Ramou, A. L. Carvalho, A. C. Roque, *Mater. Today Bio* **2022**, *15*, 100290.
- [29] Z. Wang, H. Yu, Z. Zhao, *Microchem. J.* **2021**, *169*, 106585.
- [30] H. Tao, S.-W. Hwang, B. Marelli, B. An, J. E. Moreau, M. Yang, M. A. Brenckle, S. Kim, D. L. Kaplan, J. A. Rogers, F. G. Omenetto, *Proc. Natl. Acad. Sci. U.S.A.* **2014**, *111*, 17385.
- [31] K. Chang, A. Dong, X. Yu, B. Liu, X. Zhao, R. Wang, Z. Gan, K. Jiang, Y. Niu, X. Dong, D. Zheng, Y. Li, P. Bao, Z. Zhao, H. Wang, *Adv. Electron. Mater.* **2022**, *8*, 2100843.
- [32] P. Ratanasongtham, L. Shank, J. Jakmune, R. Watanek, S. Watanek, *Chiang Mai J. Sci.* **2017**, *44*, 1431.
- [33] R. Xue, T.-F. Kang, L.-P. Lu, S.-Y. Cheng, *Appl. Sur. Sci.* **2012**, *258*, 6040.
- [34] D.-H. Kim, J. Viventi, J. J. Amsden, J. Xiao, L. Vigeland, Y.-S. Kim, J. A. Blanco, B. Panilaitis, E. S. Frechette, D. Contreras, D. L. Kaplan, F. G. Omenetto, Y. Huang, K.-C. Hwang, M. R. Zakin, B. Litt, J. A. Rogers, *Nat. Mater.* **2010**, *9*, 511.
- [35] M. S. Mannoor, H. Tao, J. D. Clayton, A. Sengupta, D. L. Kaplan, R. R. Naik, N. Verma, F. G. Omenetto, M. C. McAlpine, *Nat. Commun.* **2012**, *3*, 763.
- [36] H. Tao, M. A. Brenckle, M. Yang, J. Zhang, M. Liu, S. M. Siebert, R. D. Averitt, M. S. Mannoor, M. C. McAlpine, J. A. Rogers, D. L. Kaplan, F. G. Omenetto, *Adv. Mater.* **2012**, *24*, 1067.
- [37] D. Molinnus, K. A. Janus, A. C. Fang, A. Drinic, S. Achtsnicht, M. Köpf, M. Keusgen, M. J. Schöning, *Phys. Status Solidi A* **2022**, *219*, 2200100.
- [38] O. Garcia-Depraect, R. Lebrero, S. Rodriguez-Vega, S. Bordel, F. Santos-Beneit, L. J. Martínez-Mendoza, R. A. Börner, T. Börner, R. Munoz, *Bioresour. Technol.* **2022**, *334*, 126265.
- [39] D. Molinnus, M. Bäcker, H. Iken, A. Poghossian, M. Keusgen, M. J. Schöning, *Phys. Status Solidi A* **2015**, *212*, 1382.
- [40] U. Witt, T. Einig, M. Yamamoto, I. Kleeberg, W.-D. Deckwer, R.-J. Müller, *Chemosphere* **2001**, *44*, 289.
- [41] R. Scaffaro, A. Maio, F. Suter, E. F. Gulino, M. Morreale, *Polymers* **2019**, *11*, 651.
- [42] A. Mann, F. Lydon, B. J. Tighe, S. Suzuki, T. V. Chirila, *Biomed. Phys. Eng. Express* **2021**, *7*, 045002.
- [43] Q. Lu, B. Zhang, M. Li, B. Zuo, D. L. Kaplan, Y. Huang, H. Zhu, *Biomacromolecules* **2011**, *12*, 1080.
- [44] N. Johari, L. Moroni, A. Samadikuchaksaraei, *Eur. Polym. J.* **2020**, *134*, 109842.
- [45] Y. Ma, B. S. B. Canup, X. Tong, F. Dai, B. Xiao, *Front. Chem.* **2020**, *8*, 585077.
- [46] D. T. Pham, W. Tiyaboonchai, *Drug Delivery* **2020**, *27*, 431.
- [47] T. V. Chirila, *Int. J. Adhes. Adhes.* **2022**, *114*, 1093109.
- [48] A. Magaz, A. D. Roberts, S. Faraji, T. R. L. Nascimento, E. S. Medeiros, W. Zhang, R. D. Greenhalgh, A. Mautner, X. Li, J. J. Blaker, *Biomacromolecules* **2018**, *19*, 4542.
- [49] J. Liu, H. Chen, Y. Wang, G. Li, Z. Zheng, D. L. Kaplan, X. Wang, X. Wang, *ACS Biomater. Sci. Eng.* **2020**, *6*, 1641.
- [50] E. H. Immergut, H. F. Mark, *Plasticization and Plasticizer Processes*, Vol. 48 (Ed: N. A. J. Platzer), American Chemical Society, Washington, DC **1965**, Ch. 1.